Individual Muscle Control using an Exoskeleton Robot for Muscle Function Testing

Jun Ueda, Ding Ming, Vijaya Krishnamoorthy, Minoru Shinohara, and Tsukasa Ogasawara

Abstract— **Healthy individuals modulate muscle activation patterns according to their intended movement and external environment. Persons with neurological disorders (e.g., stroke and spinal cord injury), however, have problems in movement control due primarily to their inability to modulate their muscle activation pattern in an appropriate manner. A functionality test at the level of individual muscles that investigates the activity of a muscle of interest on various motor tasks may enable muscle-level force grading. To date there is no extant work that focuses on the application of exoskeleton robots to induce specific muscle activation in a systematic manner. This paper proposes a new method, named "individual muscle-force control" using a wearable robot (an exoskeleton robot, or a power-assisting device) to obtain a wider variety of muscle activity data than standard motor tasks, e.g., pushing a handle by hand. A computational algorithm systematically computes control commands to a wearable robot so that a desired muscle activation pattern for target muscle forces is induced. It also computes an adequate amount and direction of a force that a subject needs to exert against a handle by his/her hand. This individual muscle control method enables users (e.g., therapists) to efficiently conduct neuromuscular function tests on target muscles by arbitrarily inducing muscle activation patterns. This paper presents a basic concept, mathematical formulation, and solution of the individual muscle-force control and its implementation to a muscle control system with an exoskeleton-type robot for upper extremity. Simulation and experimental results in healthy individuals justify the use of an exoskeleton robot for future muscle function testing in terms of the variety of muscle activity data.**

I. INTRODUCTION

Healthy individuals modulate muscle activation patterns according to intended movement and environment. Persons with neurological movement disorders (e.g., stroke and spinal cord injury), however, have problems in movement control due primarily to their inability to modulate their muscle activation pattern in an appropriate manner [1], [2]. Investigation into the association between neurological impairment and a muscle-activation pattern is critical for future diagnosis and treatment since the modulated muscle-activation pattern is expected to be associated with the type and degree of impairment. The most

J. Ueda is with the George W. Woodruff School of Mechanical Engineering, Georgia Institute of Technology, Atlanta, GA 30332-0405, U.S.A. E-mail: jun.ueda@me.gatech.edu.

Ming Ding and Tsukasa Ogasawara are with the Graduate School of Information Science, Nara Institute of Science and technology, Nara 630-0192, Japan. E-mail: {min-d, ogasawar}@is.naist.jp.

V. Krishnamoorthy is with the Division of Physical Therapy, Department of Rehabilitation Medicine, Emory University, Atlanta, GA 30322, U.S.A. E-mail: vkrish3@emory.edu

M. Shinohara is with the School of Applied Physiology, Georgia Institute of Technology, Atlanta, GA 30332, U.S.A. E-mail: shinohara@gatech.edu

efficient way to find a difference in the modulation of muscle-activation pattern is to apply a unique load combination that induces a predictable modulation in the muscle-activation pattern in healthy adults while the modulation in patients is expected to be different [3]. A functionality test at the level of individual muscles may be effective, because the tests investigate the activity of a muscle of interest on various motor tasks. The functionality test would provide muscle-level information on, e.g., fatigue, impairment, and function recovery.

In the past two decades, a number of muscle-force prediction methods have been presented based on the Optimality principle [4], [5], [6], [7] that represent performance criteria on which the neuromuscular system optimizes the activation of muscle forces. Static optimization methods, dealing with isometric and relatively slow motions, predict redundant muscle forces by minimizing a cost function, comprising the sum of muscular stress or force raised to a power, subject to force/torque constraints associated with a given task. The biggest advantage is that the muscle force prediction is mathematically formulated and can be numerically solved, enabling a prediction for relatively complex tasks involving multiple joints such as walking and running. There are still arguments and criticism on the neurological background of this optimization; however, the effectiveness of this approach for predicting stereotyped motor performances has been reported in many papers [8], [9], [10], [11], [12].

To the authors' knowledge, there is no extant work that focuses on the application of exoskeleton robots to induce specific muscle activation patterns in persons applicable for muscle function testing and therapeutic planning. Due to the presence of muscle redundancy [13], joint-torques and muscle-forces are intricately coupled. This makes the planning of muscle-level function tests difficult and greatly limits the variety of function tests. Single-joint tasks, i.e., asking subjects to exert a certain joint torque, are widely performed in neuro-muscular science in order to investigate the activity of a single muscle of interest around the joint (e.g., [14]). Unfortunately, however, the number of one-to-one correspondences between a joint toque and muscle force that can be found in the human body is very limited due to the presence of biarticular muscles. Even multiple-joint tasks (e.g., [15], [16]), such as a reaching motion in the horizontal plane, are performed by adding restraints to the trunk as well as to other body parts to minimize the degrees of freedom involved and to avoid the ambiguity in the joint torque-muscle force relationship. The body restraints prevent motion; however, they do not necessarily prevent muscle activities due to reaction forces at

the restrained body parts.

This paper presents the concept of individual muscle-force control technique using an exoskeleton robot [17], [18], [19], [20]. An arbitrary muscle activation pattern is induced in subjects by performing robot-assisted motor tasks, which is expected to be applicable for future muscle function testing. The exoskeleton assists or resists the subject's joint torques during a motor task, and the subject is asked to accomplish the task by opposing the robot. The paper hypotheses that human muscle activities are determined by a physiology-based criterion function, and hence the activities of individual muscles can be predicted computationally and modulated by applying external loads by an exoskeleton. An integrated muscle-control system is developed that consists of an exoskeleton, a muscle force control solver, a human musculoskeletal human model, and a graphical interface. The planning of functionality tests at the level of individual muscles is computed by the muscle force control solver. This paper presents a closed-form solution and its proof to induce a desired muscle activity pattern based on a physiology-based criterion function. For upper-limb tasks, the amount and direction of force that a subject is asked to exert by his/her hand as well as the robot torques will be computed in a systematic manner.

The aim of this paper is to justify the efficacy of this computational approach by simulation and experiments in healthy individuals; the clinical aspects will not be investigated. The proposed method is expected to help a clinician make a comparison between stereotypical (normal) patterns and induced muscle activation patterns associated with the type and degree of impairment. Obtaining detailed diagnostic information could also help a therapist plan an appropriate therapeutic training.

II. Individual muscle-force control using an exoskeleton-type wearable robotic device

A. Motivation

For neurorehabilitation, endeffector-type robots have been used and the efficacy has extensively been investigated [21], [22], [23]. A number of exoskeleton-type robots have also been developed and used for biomedical applications [24], [25], [26], [27], [28], [29], [30], [31], [32] as well as for industry and military applications [33], [34]. Some of these exoskeleton-type robots are directly controlled by electromyographic signals (EMGs) of a wearer, which is expected to provide more intuitive and easy operation of these devices. It should be noted that the main research focus of the previous exoskeleton robots was on joint-level torque assistance or arm/foot trajectory adjustment. For example, torque commands to robot motors were determined based on the magnitude of EMG signals so that the robot can assist walking or holding a heavy weight at the joint-level[25], [28].

Investigation at the level of individual skeletal muscles is considered more appropriate and advantageous than the investigation at the level of joints, particularly in medical apprications such as muscle function diagnosis and rehabilitation of impaired muscles. The modulated muscle-activation patterns in healthy individual and person with neuromuscular

disorder are expected to be different [3]. A standard way to diagnose a muscle disorder may be to observe the activity of a muscle of interest during a motor task that specifically induces an activity in the muscle. From the observation of a muscle activity different from what is supposed to be in a healthy muscle, one would expect an impairement in the observed muscle. Also, muscle-level activities can be used to assess the efficacy of robot-assisted training on certain muscles, e.g., by EMG measurement [35] and [32].

This implies the need to plan a motor task that induces a specific muscle activation pattern in persons. A robot-assisted motor task, in particular, using a wearable exoskeleton-type robot, is favorable to obtain a wider variety of muscle activity data than conventional motor tasks, e.g., where a subject simply pushes a handle by hand. However, as suggested in [28], a muscle activity pattern induced in a subject during a robot-assisted motor task is a result of a complicated physical interaction between the subject's muscle forces and the robot's forces. The solution of this interaction problem would lead to a more sophisticated application of exoskeleton robots in terms of muscle-level force assistance/resistance for future muscle function testing. Ueda et al. have proposed the concept of individual muscle control using an exoskeleton [17], [18], [19], [20]. The key idea of this concept is to calculate the torque commands of an exoskeleton using a musculoskeletal model that mathematically solves the above-mentioned interaction problem. An desired muscle activation pattern in a selected group of human muscles (target muscles) is induced by applying torques to multiple human joints that are involved in a motor task via multiple physical interfaces of an exoskeleton robot.

B. Concept

Figure 1 shows the concept of the proposed muscle function testing using an exoskeleton. A subject is asked to wear an exoskeleton robot. The exoskeleton robot applies torques to the subject's joints to resist the movement. For example, a PC minotor displays an arrow that represents the amount and direction of a target force. The PC minotor also displays another arrow in a different color that represents the amount and direction of current force. The subject is asked to match his/her force with the instructed force *by opposing* the exoskeleton and keep the adjusted force for a while. Surface electrodes records EMG signals of target muscles. Comparisons between the recorded muscle activation patterns and stereotypical (normal) patterns would provide diagnostic information. Note that stereotypical muscle activation patterns for comparison can be computed using a musculosokeletal human model.

The influence of forces/torques applied from an exoskeleton on each individual muscle force is predicted using a human musculoskeletal model. By hypothesizing the Optimality principle in human muscle force generation, this prediction problem can be formulated as a standard constrained optimization problem introducing a cost criterion function comprising the subject's muscular stress or force raised to a power. The cost function is minimized by a numerical optimization technique

subject to the constraints associated with the force and torque requirements to perform a specific task [4], [5], [6], [7]. This research will treat this mathematical formulation for muscle-force prediction in the opposite manner; the predicted results are conversely utilized to calculate the external forces/torques from the exoskeleton robot such that a desired muscle force is induced, thereby enabling neuromuscular function test at the level of individual muscles in a "pinpointed" manner.

Mathematically, this individual muscle-force control can be regarded as a problem to determine equality constraints of the Optimality criterion such that certain desired muscle forces are obtained as a result of cost function minimization. Note that the equality constraints represent the relationship between the subject's muscle forces and joint torques. In other words, to induce a certain muscle activation pattern, corresponding joint toques need to be created by the subject where the required joint torques are calculated by the proposed algorithm. These required joint torques could be realized only by a subject's voluntary exertion of force by performing a motor-task, e.g., simply pushing a handle by hand. However, the sole change of the subject's voluntary force may be insufficient to create the required joint toques in terms of the number of control degrees of freedom (DOF). To accurately induce specific muscle activities, this paper proposed to use an exoskeleton-type robot. Recall that exoskeleton robots have a functionality to directly apply torques to the wearer's joints. The primary objective of the use of an exoskeleton is to "assist" the creation of specific joint torques in subjects. At the joint level, the exoskeleton either assists or resists the subject. The subject is asked to perform a motor task by opposing the robot. This robot-assisted motor task is expected to create a new equilibrium in the subject, resulting in inducing a desired muscle activation pattern.

C. Computational method of motor task planning for neuro-muscular function tests

The proposed motor-task planning for neuromuscular function tests computes an adequate amount and direction of a force that a subject needs to exert to induce a desired change of a target muscle force. An exoskeleton-type wearable robot is utilized to assist the change of joint torques. The overall system consists of a wearable actuator device, a handle, a muscle force control problem solver, a musculoskeletal human model, and a user-friendly graphical interface, as shown in Fig. 1. The handle to which a subject exerts a force is equipped with a force transducer and securely attached on a table. The planning and test procedure are as follows:

Step1 **Nominal muscle force prediction**: Determine the body posture and nominal task. 3D motion capture equipment may be used to record the joint angles if necessary. The musculoskeletal human model calculates nominal muscle forces by Static Optimization.

Step2 **Designation of muscle forces**: Using the graphical user interface, designate target muscle(s) and determine the change ratios of forces based on the nominal muscle forces.

Step 3 **Motor task planning**: The muscle force control solver checks the feasibility of the designated muscle forces in terms of the Principle of Optimality. The force that the subject needs to exert to the handle is calculated. Control commands to the exoskeleton robot are calculated if needed.

Step 4 **Task execution**: The exoskeleton robot applies joint torques. An instruction monitor displays the computed force using an arrow and the current force using another arrow. Subjects perform a force-matching task to match the hand-force with the instructed force and keep the adjusted force for a while, resulting in inducing the desired changes of the target muscle forces.

Step 5 **Evaluation**: Comparisons between the recorded muscle activation pattern and stereotypical (normal) pattern will be made. The stereotypical muscle activation pattern is computed using the musculoskeletal human model.

This paper presents a theoretical formulation and solution of Step 1–3. Step 4 is validated by simulation and experiments in health individuals. Step 5 including the study of the clinical aspects is not considered.

III. MUSCLE-FORCE CONTROL SYSTEM

A. Musculoskeletal model

A musculoskeletal model of the human upper-right limb shown in Fig. 2(a) was developed [18] to calculate moment-arms to attached bones for each of the muscles. This model consists of 5 rigid links with 12 joints corresponding to the waist, neck, shoulder, elbow, and wrist joints. Massless-wires model a total 51 muscles of the upper-right limb in Table I according to [8], [12], [36]. The points of muscle attachment (origins and insertions) are determined from anatomical data [12]. In [18], this musculoskeletal model was evaluated in terms of muscle moment arms [37].

In this paper, a total of 9 joints from the torso to wrist will be considered as shown in Fig. 2(b). By applying the Static Optimization method (e.g., Crowninshield's method, see Appendix A), the redundant muscle forces can be predicted by minimizing a cost function for static tasks or relatively slow (i.e., quasi-static) motions. This model is used to compute the interaction between the human muscle forces and forces generated by the exoskeleton robot. In addition, the predicted results can be considered as stereotypical muscle activities that healthy individuals are supposed to generate. The comparison between induced muscle activation patterns in subjects and computed patterns is expected to provide some useful diagnostic information.

B. Exoskeleton robot

A wearable robotic device using pneumatic actuators shown in Fig. 3(a) has been developed to control the muscle forces of the human upper-right limb. Figure 3(b) shows the structure of the robot. This device applies 4 degrees of freedom of torques (DOFs) of the right arm: 1 DOF for the flexion/extension of the elbow joint, 1 DOF for the supination/pronation of the forearm, and 2 DOF for the flexion/extension and adduction/abduction of the wrist joint, by a total of 8 actuators. The
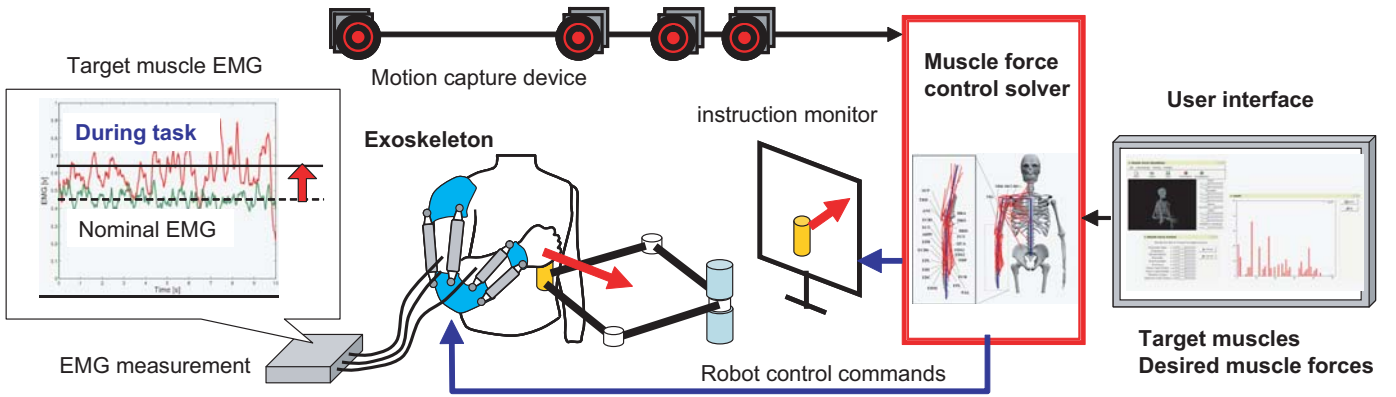
Fig. 1.   Muscle function test using an exoskeleton robot: A subject performs a robot-assisted motor task as instructed by a PC monitor. An exoskeleton robot either assists or resists the subject's joint torques. 3D motion capture and electromyographic equipment collect data during a task.

TABLE I
LIST OF MUSCLES IN MUSCULOSKELETAL MODEL

No.	Muscle Name	No.	Muscle Name	No.	Muscle Name	No.	Muscle Name
1	Levator Scapulae	14	Latissimus dorsi medial	27	Brachialis	40	Pronator Quadratus
2	Pectoralis major up	15	Latissimus dorsi lower	28	Brachioradialis	41	Abductor Pollicis Longus
3	Pectoralis major low	16	Subscapularis	29	Triceps long	42	Pronator teres
4	Pectoralis minor	17	Deltoideus anterior	30	Triceps lateral	43	Extensor Carpi Ulnaris
5	Subclavius	18	Deltoideus lateral	31	Triceps short	44	Extensor Carpi Radialis
6	Serratus ant.upper	19	Deltoideus post	32	Anconeus	45	Extensor Carpi Radialis
7	Serratus ant.lower	20	Supraspinatus	33	Flexor Carpi Ulnaris	46	Common Digital Extensor
8	Trapezius upper	21	Infraspinatus	34	Flexor Carpi Radialis	47	Extensor Digiti Minimi
9	Trapezius medial	22	Teres major	35	Palmaris Longus	48	Extensor Indicis
10	Trapezius lower	23	Teres minor	36	Flexor Digitorum Superficialis	49	Extensor Pollicis Longus
11	Rhomboids upper	24	Coracobrachial	37	Flexor Digitorum Superficialis	50	Extensor Pollicis Brevis
12	Rhomboids lower	25	Biceps long	38	Flexor Digitorum Profundus	51	Supinator
13	Latissimus dorsi upper	26	Biceps short	39	Flexor Pollicis Longus		

pneumatic actuator shown in Fig. 3(a) with 20 [mm] diameter, maximum pressure of 0.4 [MPa], and maximum force of 60 [N] is used. Each of the actuators is equipped with a force transducer as shown in Fig. 4 and controlled by a combination of feed forward and feedback (Proportional-integral force feedback) control. This actuator contracts when pressurized by a compressor controlled by an electropneumatic regulator. The actuators are also modeled as wires and integrated with the human kinematic model as shown in Fig. 3(c). At this point, this device does not have actuators to apply torques to the 3 DOF of the shoulder joint. The shoulder mechanism will be added in the near future. Both ends of each actuator are attached to plastic frames through attachments which are then attached to the body by Velcro tapes. The adjustment holes on the actuator attachments provide the adaptability to difference body sizes. The total weight of the exoskeleton including 8 pneumatic actuators, 8 force transducers, attachment frames, and tubings is 2.5 kg, which excludes pneumatic servo valves and a compressor.

Although this paper refers this robotic device as "exoskeleton", this device, unlike other exoskeleton mechanisms, does not have any rigid link mechanisms but only compliant pneumatic actuators for safety reasons. The maximum pressure of the compressor is limited so that the maximum force generated by a single actuator does not exceed 60N. This force reduces as an actuator contracts and becomes 0N for around 12% of contraction. Therefore, the torques applied by

the exoskeleton will reduce if the subject moves his/her joints along the directions of the applied forces, leading to weaker application of torques. The actuators are made from compliant rubber that does not require protective covers. In addition, no rigid member connects a joint to another; only actuators are connecting the joints, hence the movement of a subject is not kinematically constrained. Even though all the actuators exert their maximum forces, the aggregate joint torque generated by the robot is not strong so that a subject can move his/her joints by resisting the exoskeleton robot.
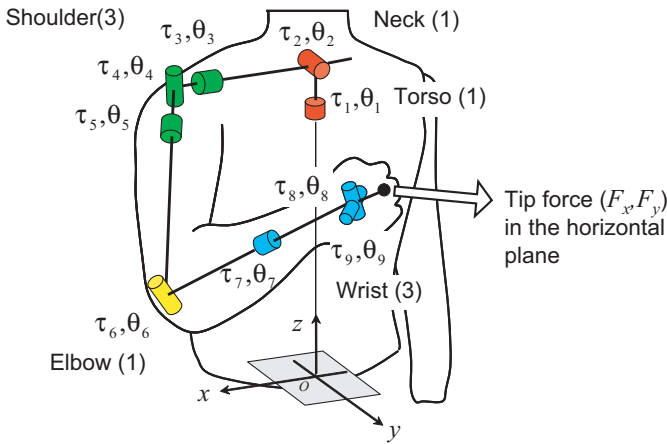
For generating the feed forward command, the characteristic of the pneumatic actuator is modeled by linear approximation. The force p created by the actuator is calculated simply by Hooke's law:

$$p = \eta(l - l_{\text{free}}(P)), \qquad (1)$$

where P is the air pressure controlled by an electropneumatic regulator, $l_{\text{free}}(P)$ is a neutral length of the actuator as a function of the air pressure, and l is the actual length of the actuator. η is a spring constant of the actuator. As shown in Fig. 5(a), the neutral length $l_{\text{free}}(P)$ can be approximated by a linear function. In addition, as can be observed in Fig. 5(b), the spring constant, i.e., the gradient of each displacement-force relation, does not largely change for the change of air pressure, implying that a constant η may be used for the modeling. A brief procedure to determine an air pressure P is as follows: By using a motion capture system, the joint angles of a subject are obtained. These joint angles are given
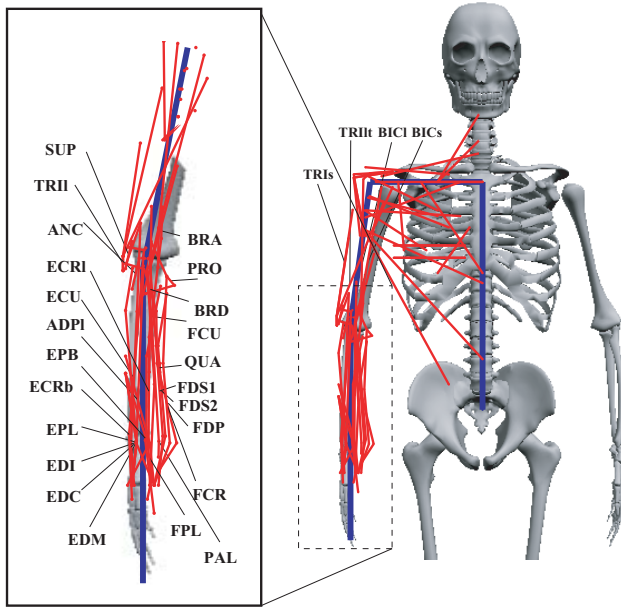
(a) 51 Muscles modeled in the musculoskeletal model (not all of them are labeled)[18]
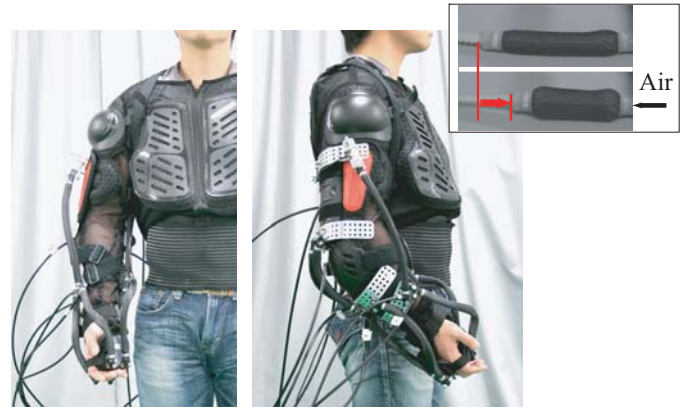

(b) Joint configuration

Fig. 2.   Human musculoskeletal model of the Upper-right limb

(a) Wearable exoskeleton robotic device with 8 pneumatic actuators: No rigid link mechanism connect joints. The total weight is 2.5 kg.
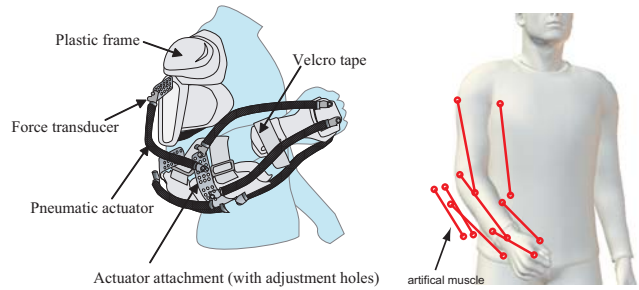
(b) Robot structure

(c) Robot kinematic model:

Fig. 3.   Exoskeleton robot and kinematic model
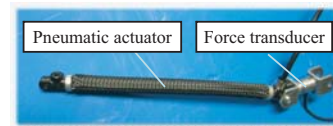
Fig. 4.   Control of a pneumatic actuator: A force transducer connected in series provides feedback force control.

to the kinematic model of the robot that outputs current lengths of individual pneumatic actuators. The current length of each actuator, i.e., l, is used to calculate P to realize a desired force p based on (1). This P is used for the feedforward control. The feedback control will compensate for unmodeled nonlinear and dynamic characteristics of the actuator. The force controller settles within 15 seconds to a constant reference force.

C. Muscle-force control solver

The muscle-force control solver described later computes an adequate amount and direction of force that a subject needs to exert, e.g., by his/her hand, to induce the desired muscle forces of the target muscle forces. The solver also computes joint torques that the exoskeleton robot applies to the subject's

joints if the exertion of force by the subject is not sufficient, and therefore additional torque control is required. A graphical user-interface provides an easy operation to designate desired forces for target muscles, and to view the distribution of resultant muscle forces.

IV. PROBLEM FORMULATION AND SOLUTION

A. Static equation

In this paper, the individual muscle-force control for static tasks is considered; we assume that a subject does not change his/her posture during a task and all muscle contractions are isometric. The dynamics of the body and exoskeleton robot is neglected. Consider a human musculoskeletal model that has M joints and N muscles. The static equation of this musculoskeletal system (e.g., see Fig. 2(b)) is given by
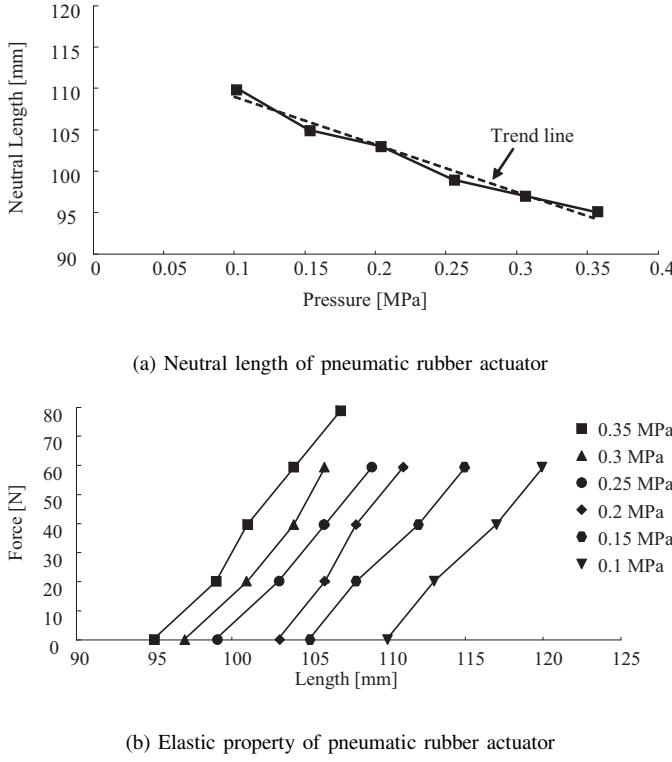
(a) Neutral length of pneumatic rubber actuator

(b) Elastic property of pneumatic rubber actuator

Fig. 5.   Characteristics of Pneumatic Rubber Actuator

$$\begin{aligned}
\boldsymbol{\tau}_h &= \boldsymbol{g}(\boldsymbol{\theta}) + \boldsymbol{J}(\boldsymbol{\theta})^T \boldsymbol{F} - \boldsymbol{\tau}_a = \boldsymbol{A}(\boldsymbol{\theta})\boldsymbol{f} \\
&= \begin{bmatrix} a_{11} & \cdots & a_{1N} \\ \vdots & \ddots & \vdots \\ a_{M1} & \cdots & a_{MN} \end{bmatrix} \begin{bmatrix} f_1 \\ \vdots \\ f_N \end{bmatrix}.
\end{aligned} \quad (2)$$

where $\boldsymbol{\tau}_h \in \Re^M$ is the human joint torque vector, $\boldsymbol{\theta} = [\theta_1, \cdots, \theta_M]^T \in \Re^M$ is the joint angle vector, $\boldsymbol{F} = [F_x, F_y, F_z]^T$ is the translational force at the tip, $\boldsymbol{J}(\boldsymbol{\theta})$ is the Jacobian between the tip-force and joint torques, $\boldsymbol{g}(\boldsymbol{\theta})$ is the gravity force, $\boldsymbol{\tau}_a \in \Re^M$ is the joint torque generated by the exoskeleton robot, $\boldsymbol{A} \in \Re^{M \times N}$ is the moment-arm matrix of the muscles, and $\boldsymbol{f} = [f_1, \cdots, f_N]^T \in \Re^N$ is the human muscle force vector. The element a_{ij} of $\boldsymbol{A}$ denotes the moment arm of muscle j for joint i. $a_{ij} = 0$ is given if f_j does not affect on joint i. Note $f_j \geq 0 \ (j = 1, \cdots, N)$ because of muscle contraction. $\boldsymbol{g}(\boldsymbol{\theta})$, $\boldsymbol{J}(\boldsymbol{\theta})$, and $\boldsymbol{A}(\boldsymbol{\theta})$ for a given posture $\boldsymbol{\theta}$ can be calculated by the musculoskeletal model in Fig. 2(a). To simplify the problem, we assume that the robot can produce joint torques without any mechanical limitations.

B. Static optimization

The human body has a redundant number of muscles than the number of joints, i.e., $N >> M$. This fact makes the prediction of muscle forces $\boldsymbol{f}$ by knowing joint torques $\boldsymbol{\tau}_h$ an ill-posed problem. Various optimization approaches have been proposed to model the Principle of Optimality [4], [5], [6], [7] and to solve this problem by minimizing a cost function. The main difference among the approaches is the structure of cost functions that represent performance criteria on which the neuromuscular system optimizes the activation of muscle forces. In much literature that deals with isometric or relatively slow motions, the cost functions have a general form comprising the sum of muscular stress or force raised to a power. The static optimization method can be formulated as follows.

$$\text{Minimize} \quad u(\boldsymbol{f}) = \sum_{j=1}^{N} c_j f_j^r \quad (3)$$

$$\text{subject to} \begin{cases} \boldsymbol{\tau}_h = \boldsymbol{A}\boldsymbol{f} \\ 0 \leq f_j \leq f\max_j (j = 1, \cdots, N) \end{cases}$$

where $u(\boldsymbol{f})$ is a cost function, c_j's are weighting factors, and r is an integer number. It should be noted that arguments still exist on the choice of the weighting factors c_j and the integer r of the power [4], [5], [6], [7]. This research will treat this general form of cost functions "as is" since it provides a sufficient form for mathematical analysis. The different choice of parameters can be treated easily in numerical calculation. Therefore, the muscle force control technique is expected to be applicable for any static optimization criteria.

C. Formulation of individual muscle force control

Excluding direct stimulation of individual muscles, muscle forces are indirectly controlled through the modification of joint torques. Technically speaking, even if the exoskeleton robot device assists the modification of joint torques by applying external torques, the total number of joints (i.e., control inputs) is much fewer than the number of muscles (i.e., control outputs). Since we hypothesize that human muscle forces obey the Optimality principle, a distribution of muscle forces against the principle can never be realized. As described earlier, the exoskeleton robot device merely modifies the human joint torques, which is equivalent to the modification of the equality condition of the cost minimization in (3). In other words, the proposed pinpointed muscle force control is an indirect control of muscle forces by an appropriate modification of the equality condition for cost function optimization.

Let $\boldsymbol{f}_0$ be the nominal muscle forces obtained in Step 1 in Section II-C. Based on the nominal muscle forces, the N muscles are classified into two groups: active muscles and inactive muscles. The active muscles correspond to the elements having nonzero values in $\boldsymbol{f}_0$, and the inactive muscles correspond to zero elements. Let $\tilde{N} \leq N$ be the number of the active muscles, and $N - \tilde{N}$ be the number of the inactive muscles. In the muscle-force control, the inactive muscles' forces are kept inactive. The active muscles are further divided into two portions: **target muscles** $\boldsymbol{f}_t \in \Re^{N_t}$ and **non-target muscles** $\boldsymbol{f}_n \in \Re^{N_n}$ where $N_t + N_n = \tilde{N}$. Without the loss of generality, the order of the N muscles may be permuted according to these three groups for the simplicity of description:

$$\boldsymbol{f} \triangleq \begin{bmatrix} \boldsymbol{f}_t \\ \hline \boldsymbol{f}_n \\ \hline \boldsymbol{0} \end{bmatrix} \begin{array}{l} \cdots \text{target muscles} \\ \cdots \text{non-target muscles} \\ \cdots \text{inactive muscles} \end{array} \quad (4)$$

The desired muscle forces $\boldsymbol{f}_{td}$ are given as follows by explicitly specifying the change ratio for each of the target muscles:

$$\boldsymbol{f}_{td} = \text{diag}[\gamma_1, \gamma_2, \cdots, \gamma_{N_t}]\boldsymbol{f}_{t0} \tag{5}$$

where $\gamma_j(> 0)$ is the change ratio of the j-th target muscle. Hereafter the subscript d denotes the desired muscle forces, and 0 denotes the nominal muscle forces. The above permutation for $\boldsymbol{f}$ is also applied to the moment-arm matrix $\boldsymbol{A}$ accordingly:

$$\boldsymbol{A}^T = \left[\begin{array}{c} \boldsymbol{A}_t \\ \hline \boldsymbol{A}_n \\ \hline \boldsymbol{A}_v \end{array} \right] \begin{array}{l} \cdots \text{target muscles} \\ \cdots \text{non-target muscles} \\ \cdots \text{inactive muscles} \end{array} \tag{6}$$

Hereafter these permuted vectors and matrices will be used.

The muscle-force control is to obtain the tip-force $\boldsymbol{F}$ that a subject exerts against the handle and the external torques $\boldsymbol{\tau}_a$ that the exoskeleton robot generates. Define the total external torque vector $\boldsymbol{\tau}_{ex} \in \Re^M$ as the sum of the torques created by the reaction force of $\boldsymbol{F}$ and the exoskeleton's torque $\boldsymbol{\tau}_a$:

$$\boldsymbol{\tau}_{ex} = \boldsymbol{J}^T\boldsymbol{F} - \boldsymbol{\tau}_a \tag{7}$$

The mathematical formulation of the muscle-force control is given as follows:

$$\boldsymbol{f}_{td} = \left[\begin{array}{cc} \boldsymbol{I}^{N_t \times N_t} & \boldsymbol{O}^{N_t \times (N-N_t)} \end{array} \right] \underset{\boldsymbol{\tau}_{ex}}{\arg\min} \sum_{j=1}^{N} c_j f_j^r, \tag{8}$$

where the first term is a selection matrix.

D. Solution of individual muscle-force control

The solution of the above-mentioned muscle-force control is not straightforward while many numerical optimization packages are applicable for muscle force prediction. Applying optimality conditions for constrained optimization problems such as those given in the Karush-Kuhn-Tucker (KKT) conditions [38], [39] can analytically solve the problem.

Since the number of control inputs (i.e., the number of the elements of $\boldsymbol{\tau}_{ex}$) is limited, the priority-based approach is applied. The first priority is to exactly realize the desired forces $\boldsymbol{f}_{td}$ of the target muscles. The second priority is to minimize the changes of the non-target muscles since the non-target muscle forces will be influenced by the first-priority muscle control due to the physical coupling among the muscles.

Theorem: The external torque $\boldsymbol{\tau}_{ex}$ as the solution of (8) is given by

$$\boldsymbol{\tau}_{ex} = \left[\boldsymbol{A}_t^T\ \boldsymbol{A}_n^T\right] w^{-1}\left(\left[\begin{array}{c} \boldsymbol{A}_t \\ \boldsymbol{A}_n \end{array} \right] \boldsymbol{\alpha} \right) \tag{9}$$

where $w(*)$ is a function that converts the muscle force vector $\boldsymbol{f}$ to a new vector $\boldsymbol{q}$ as $\boldsymbol{q} = w(\boldsymbol{f})$ where the j-th elements of $\boldsymbol{f}$ and $\boldsymbol{q}$ have the following relationship:

$$q_j \triangleq \frac{\partial u(\boldsymbol{f})}{\partial f_j} = rc_j f_j^{r-1}, (j = 1, \cdots, N). \tag{10}$$

$\boldsymbol{f} = w^{-1}(\boldsymbol{q})$ is the inverse function of $w(*)$. Also, $\boldsymbol{\alpha}$ is given as $\boldsymbol{\alpha} = \boldsymbol{A}_t^+ [w(\boldsymbol{f}_{td}) - w(\boldsymbol{f}_{t0})] + (\boldsymbol{I} - \boldsymbol{A}_t^+\boldsymbol{A}_t)\boldsymbol{\beta}$,

where $\boldsymbol{I}$ is the identity matrix, and $\boldsymbol{\beta}$ is a free parameter that represents the remaining redundancy for controlling the non-target muscles as the second priority. To minimize the influence on the non-target muscles in terms of the root-mean-square (RMS) change, $\boldsymbol{\beta}$ is given as $\boldsymbol{\beta} = \left[-\boldsymbol{A}_n(\boldsymbol{I} - \boldsymbol{A}_t^+\boldsymbol{A}_t)\right]^+ \boldsymbol{A}_n\boldsymbol{A}_t^+ [w(\boldsymbol{f}_{td}) - w(\boldsymbol{f}_{t0})]$. **Proof**: See Appendix B.

The computed net joint torque in (9) is realized by an appropriate choice of $\boldsymbol{F}$ and $\boldsymbol{\tau}_a$ (see (7)). It should be noted that (7) and (9) imply the necessity of the use of an exoskeleton-type robot to realize a desired muscle activation pattern; the sole application of the subject's voluntary force (i.e., the choice of the three parameters in $\boldsymbol{F} = [F_x, F_y, F_z]^T$ for conventional motor tasks) may not be sufficient in terms of the number of control degrees of freedom when $M > 3$. For example, additional joint torque control by the exoskeleton is necessary since $M = 9$ in the musculoskeletal model shown in Fig. 2(a) to realize $\boldsymbol{f}_{td}$. The simulation section V will validate the value of the use of the exoskeleton to obtain a wider variety of muscle activation patterns than performing conventional motor tasks. This also indicates that there exists a certain freedom for determining $\boldsymbol{F}$ and $\boldsymbol{\tau}_a$ at the level of joint torque. The simulation section will determine $\boldsymbol{F}$ and $\boldsymbol{\tau}_a$ from a practical point of view.

E. Feasibility conditions

The existence of $\boldsymbol{\alpha}$ for given $\boldsymbol{f}_{td}$ can be checked by the following three conditions.

1) $\boldsymbol{f}_{td}$ for the target muscles is completely realized if $\text{rank}(\ \boldsymbol{A}_t\ ) = \text{rank}(\ \left[\begin{array}{cc} \boldsymbol{A}_t & w(\boldsymbol{f}_{td}) - w(\boldsymbol{f}_{t0}) \end{array} \right]\ )$.
2) The inactive muscles keep inactive if

$$-\boldsymbol{A}_v \left[\begin{array}{c} \boldsymbol{A}_t \\ \boldsymbol{A}_n \end{array} \right]^+ \left[\begin{array}{c} \boldsymbol{q}_{t0} \\ \boldsymbol{q}_{n0} \end{array} \right] - \boldsymbol{A}_v\boldsymbol{\alpha} > 0. \tag{11}$$

3) The resultant muscle forces of the non-target muscles remain positive if $\boldsymbol{A}_n\boldsymbol{\alpha} + w(\boldsymbol{f}_{n0}) > 0$.

Proof: See Appendix B. Note that each of the conditions has a physiological meaning. If all of the conditions are not satisfied, the control of the designated target muscles for given $\boldsymbol{f}_{td}$ is not physiologically realizable, i.e., the violation of the Principle of Optimality. Therefore, the change ratios of the target muscle forces or the choice of the target muscles must be modified.

V. SIMULATION

A. Increasing muscle force variation by the exoskeleton

Consider a motor task where a subject is statically holding a weight (iron dumbbell), i.e., $\boldsymbol{F} = [0, 0, F_z]^T$. Figure 6 (a) shows the muscle force prediction result for muscles FCU (No. 33) and ECU (No. 43) for 5 different weights without the use of the exoskeleton. The Crowninshield's cost function is applied for the Optimality criterion (see Appendix A).

As shown in Figure 6 (a), the forces of FCU and ECU are linearly coupled. This one-to-one correspondence between the two muscles implies that this standard motor task (i.e., holding a weight) does not create rich muscle force activity data in terms of individual muscle forces. However, the application
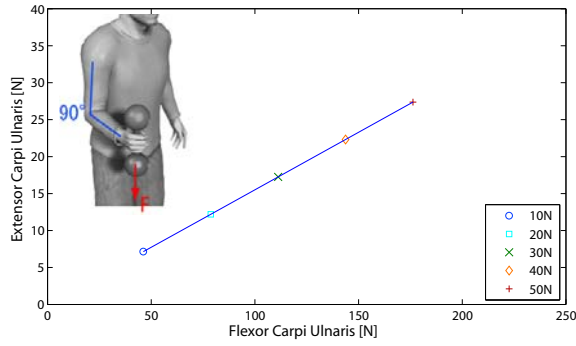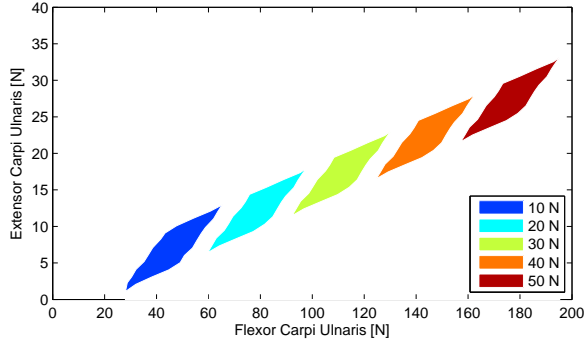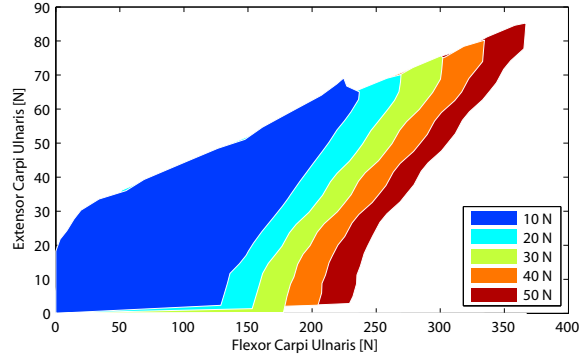
(a) Without exoskeleton

(b) With exoskeleton: Exoskeleton applies torques $\pm 0.15 \text{N} \cdot \text{m}$ to joints τ_1 to τ_9

(c) With exoskeleton: Exoskeleton applies torques $\pm 1.5 \text{N} \cdot \text{m}$ to joints τ_1 to τ_9

Fig. 6. Increasing variation in the relationship between Flexor Carpi Ulnarismuscle (33) and Extensor Carpi Ulnaris muscle (43) using an exoskeleton: Robot-assisted motor-tasks in which the subject performs a motor task by opposing the robot provides a wider variety of muscle activities.

of the exoskeleton robot increases the variation of muscles forces. Figure 6 (b) shows the result where the exoskeleton robot applies torques between -0.15 and $0.15 \text{N} \cdot \text{m}$ to joints τ_1 to τ_9. The variation can be further increased by increasing the joint torques. Figure 6 (c) shows the result for the assist torques between -1.5 and $1.5 \text{N} \cdot \text{m}$ for joints τ_1 to τ_9.

B. Motor task planning

Example 1 (Tasks A–C): The proposed algorithm computes the robot torques and tip-forces to induce a given muscle activation pattern. Tasks A–C in Table II are considered for the nominal muscle forces in which a subject is exerting a tip-force of $\boldsymbol{F} = [0, 0, F_z]^T = [0, 0, 10]^T[\text{N}]$ to hold a weight.

TABLE II
TARGET MUSCLES AND DESIRED FORCES [N] (CHANGE RATIOS) FOR
BRACHIORADIALIS(BRA), FLEXOR CARPI ULNARIS(FCU), AND
EXTENSOR CARPI ULNARIS(ECU)

Muscle	Nominal	Task		
		A	B	C
BRA	19.3	38.5 (x2.0)	9.6 (x0.5)	28.9 (x1.5)
FCU	46.2	37.0 (x0.8)	55.5 (x1.2)	92.4 (x2.0)
ECU	7.1	3.6 (x0.5)	8.6 (x1.2)	14.3 (x2.0)

Robot torques are computed as shown in Table III to realize the desired changes for the three target muscles, Brachioradialis(BRA), Flexor Carpi Ulnaris(FCU), and Extensor Carpi Ulnaris(ECU), without the change of the weight at the tip.

Example 2 (Task D): Consider the same nominal task. Next a motor-task that realizes a desired force (change ratio) for each of the following 7 target muscles will be considered: Subclavius: 1.4 [N] ($\times$ 0.9), Biceps long: 13.0 [N] ($\times$ 1.3), Biceps short: 40.0 [N] ($\times$ 1.3), Brachioradialis: 23.0 [N] ($\times$ 1.2), Flexor Carpi Ulnaris: 65.0 [N] ($\times$ 1.4), Pronator teres: 9.9 [N] ($\times$ 1.2) , Extensor Carpi Ulnaris: 6.5 [N] ($\times$ 0.9). For this task, assist torques and tip-forces $\boldsymbol{F} = [F_x, F_y, F_z]^T$ are simultaneously computed as shown in Table III.

Figure 7 (a) shows the planned tip-force for Task D and induced changes of the muscle forces. The arrow in the figure indicates the direction of the tip-force that the subject is asked to apply to a handle. At the same time, the exoskeleton robot applies torques to the subject's joints as shown in the bottom row of Table III. The changes of muscle forces from the nominal task to planned Task D are also shown by color in the figure. The colors represent the amount of the change of the muscle forces from the nominal forces. Red color indicates that the force of a corresponding muscle became greater than the one of the nominal task. Blue indicates that the force became smaller than the nominal task.

As observed in Figure 7 (b), the target muscles are perfectly controlled as desired, which justifies the obtained closed-form solution. Note that all the Tasks A–D satisfy the feasibility conditions in Section IV-E. Recall the Extensor Carpi Ulnaris muscle controlled in Tasks is known as a biarticular muscle, working on both the wrist and the elbow joints. The proposed method models the complex coupling between the joint-torques and muscle-forces including biarticular muscles and computes an adequate task. With the increased number of joints that are influenced by a motor task, the proposed approach becomes more effective, leading to obtaining a wider variety of muscle activity data.

VI. EXPERIMENTS

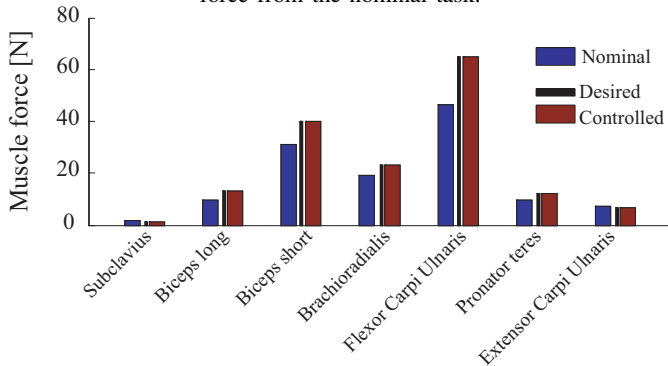#### A. Validation of muscle force prediction during motor tasks

First, the accuracy of muscle force prediction using the developed musculoskeletal model is experimentally checked for 8 healthy male subjects. Subjects hold a weight with their right hand for a posture shown in Fig. 8 without the use of the exoskeleton and surface electromyographic signals (EMGs) are recorded for Brachialis (BRA, No.27), Brachioradialis (BRD, No.28), and Flexor Carpi Ulnaris (FCU, No. 33)

TABLE III
COMPUTED TIP-FORCES AND ASSIST-TOQUES FOR TASKS A –D

Task	Assist torque [N ·m]									Tip-force [N]		
	τ_1	τ_2	τ_3	τ_4	τ_5	τ_6	τ_7	τ_8	τ_9	F_x	F_y	F_z
A	0.00	0.00	0.27	-0.04	-0.03	-3.16	0.39	-0.05	0.11	0.00	0.00	10.00
B	0.00	0.00	-0.14	0.02	0.02	1.47	-0.20	-0.04	-0.17	0.00	0.00	10.00
C	0.00	0.00	-0.23	0.05	0.03	-1.40	-0.86	-0.07	-0.67	0.00	0.00	10.00
D	0.00	0.00	1.87	1.33	0.05	-1.42	0.07	-0.21	-0.40	-1.82	0.15	10.00
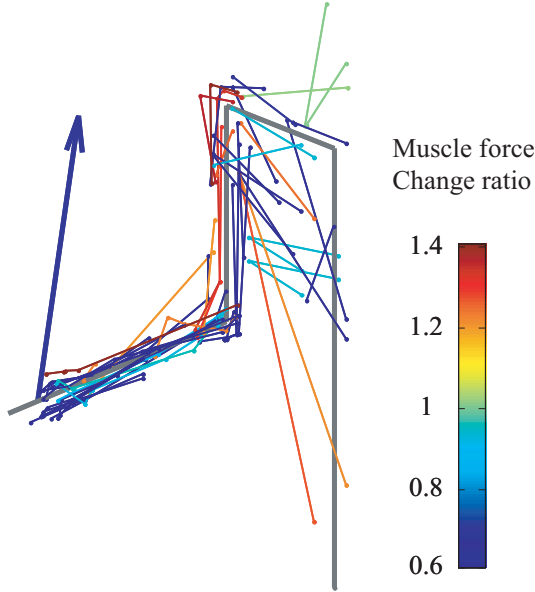
(a) Muscle force change ratio and planned tip-force: The arrow indicates the direction of the tip-force to induce the speficied changes in the target muscles. Color indicates the change of muscle force from the nominal task.

(b) Controlled muscle force
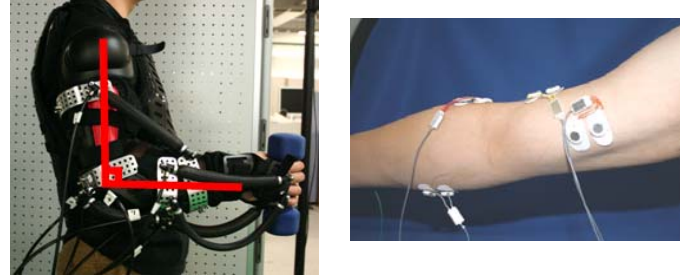
Fig. 7. Simulation result of Example 2 (Task D)

Fig. 8. Muscle Force Control Experiment: Posture (with the exoskeleton) and EMG measurement
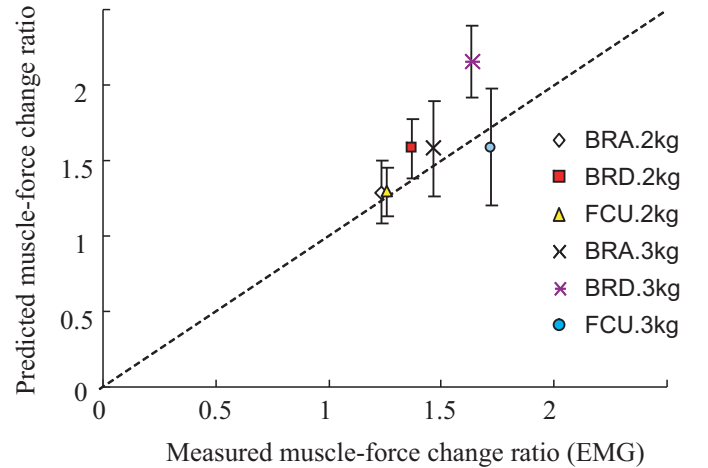

Fig. 9. Validation of Muscle Force Prediction: Normalized by predicted/measured forces when holding 1kg weight.

Although the accuracy of muscle force prediction might be improved by taking the individual differences into account such as moment arms, physiological cross sectional areas, etc., we judge that the obtained accuracy is comparative to previous studies and acceptable for this study.

B. Validation of individual muscle-force control

Muscle force control experiments for the same posture as shown in Fig. 8 were conducted by using the exoskeleton device. The target muscles are Brachialis (No.27), Brachioradialis (No.28), and Externsor Carpi Ulnaris (No.43). The desired ratios of change are given as shown in Table IV. For example, Experiment A is to support only Externsor Carpi Ulnaris, Experiment C is to support only Brachialis and Brachioradialis, and Experiment E is the mixture of assisting and resisting. Since Brachialis and Brachioradialis are physiologically coupled, these two muscles are treated as

muscles. The changes of the EMG signals are calculated when holding a weight of 2kg and 3kg respectively based on the signals when holding a weight of 1kg. The corresponding tasks are simulated by using the developed musculoskeletal model and the changes of muscle forces are predicted.

Figure 9 plots the changes of the measured EMG signals versus the corresponding predicted changes for a total of 6 tests (3 muscles × 2 types of weights). Plots closer to the dashed line validate the prediction. The average error among the 6 tests was 9.9% and the maximum error was 24.3% for the Brachioradialis muscle when holding the weight of 3 kg.

TABLE IV
DESIRED RATIOS OF CHANGE FOR EXPERIMENTS

No.	Name	Experiment				
		A	B	C	D	E
27	Brachialis	x 1.0	x 1.0	x 0.5	x 0.5	x 0.5
28	Brachioradialis	x 1.0	x 1.0	x 0.5	x 0.5	x 0.5
43	Extensor Carpi Ulnaris	x 0.5	x 1.3	x 1.0	x 0.5	x 1.3

a group, giving the same ratio of change. The feasibility for all the five experiments has been confirmed.

Each experiment is conducted for 6 healthy male subjects. Figure 10 shows the results. The light gray bars show the desired changes of the target muscles and the dark gray bars show the changes of the measured EMGs based on the nominal cases without the use of the exoskeleton. As observed in the graphs, all the tendencies of the change among the EMGs are as expected, which validates the efficacy of the proposed method. For example, in Experiment D, all the target muscle forces reduced accordingly. Similarly, both Brachialis and Brachioradialis reduced, and Externsor Carpi Ulnaris increased in Experiment E, implying that even the mixture of assisting and resisting has been realized not only by simulation but also by experiment. Note that surface EMG signals are not accurate enough to precisely evaluate the accuracy of the archived changes since the relation between the magnitude of muscle force and the one of the corresponding EMG signal is not necessarily linear. In our future work, needle EMG signals will be used for more accurate evaluation.

VII. CONCLUSION

This paper has presented the concept of individual muscle-force control and its application to a motor task planning for neuromuscular function tests using an exoskeleton-type robot. The presented algorithm computed an adequate amount and direction of force that a subject needs to exert by his/her hand to induce designated changes of the target muscles. The simulation results have confirmed the validity of the analytical solution as well as justified the use of the exoskeleton robot in terms of the variety of muscle activity data. The experimental validation by recording surface electromyographic signals (EMGs) in healthy individuals has also been conducted. Future work includes 1) improvement of control accuracy, 2) validation of the efficacy for various motor tasks, 3) integration of a more efficient and user-friendly system, and 4) experimental investigation of the applicability to dynamic motor-tasks.

The robot-assisted motor tasks could help a clinician differentiate induced muscle activation patterns in patients from stereotypical patterns by inducing arbitrary muscle activation patterns in a pinpointed manner. The exoskeleton robot is expected to contribute to induce a wider variety of muscle activities than performing conventional motor-tasks. The obtained diagnostic information could help a therapist effectively plan a tailored therapy for a specific disorder. The future work also includes the investigation of the clinical aspects of this method. The proposed method could also be applicable to sport science; to examine the effectiveness of a training machine to train a certain group of muscles, to plan effective physical training, and to design new training instruments.
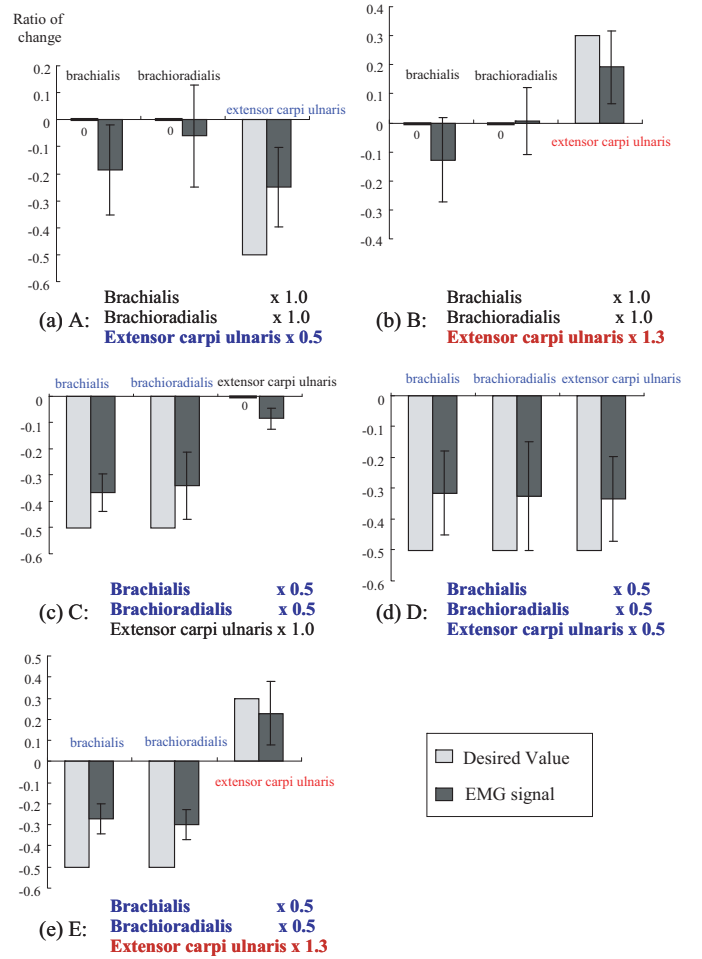

Fig. 10.   Experimental Results: Ratio of change

APPENDIX A
CROWNINSHIELD'S STATIC OPTIMIZATION

Crowninshield's method [4] predicts human muscle forces by minimizing a physiologically based criterion $u(\boldsymbol{f})$:

$$u(\boldsymbol{f}) = \sum_{j=1}^{N} \left(\frac{f_j}{\text{PCSA}_j} \right)^r \to \min \qquad (12)$$

$$\text{subject to} \quad \begin{cases} \boldsymbol{\tau}_h = \boldsymbol{A}\boldsymbol{f} \\ f_{\min j} \leq f_j \leq f_{\max j} (j = 1, \cdots, N) \end{cases},$$

where PCSA_j is the physiological cross sectional area (PCSA), and $f_{\max j} = \varepsilon \cdot \text{PCSA}_j$ is the maximum muscle force of the j-th muscle. In this paper, $\varepsilon = 0.7 \times 10^6 [\text{N/m}^2]$ is given according to [9]. PCSA_j's are given according to [40]. $f_{\min j} = 0, \forall j$ and $r = 2$ are used. See [4] for the choice of r.

APPENDIX B
PROOF OF MUSCLE-FORCE CONTROL

The feasibility of the muscle-force control is examined as follows by formulating the problem as a constrained optimization problem. For simplicity, the right side of the inequality condition $f_j \leq f_{\max j}$ $(j = 1, \cdots, N)$ is neglected and only the condition $0 \leq f_j$ is considered. Since $\boldsymbol{f}$ is a solution of (3), it must satisfy Kuhn-Tucker theorem [38], [39]:

$$\nabla u(\boldsymbol{f}) + \sum_{i=1}^{M} \mu_i \nabla h_i(\boldsymbol{f}) + \sum_{j=1}^{N} \lambda_j + \nabla g_j(\boldsymbol{f}) = 0, \quad (13)$$

$$h_i(\boldsymbol{f}) = 0 \quad (i = 1, \cdots, M), \quad (14)$$

$$\lambda_j g_j(\boldsymbol{f}) = 0, \lambda_j \geq 0, g_j(\boldsymbol{f}) \leq 0 \ (j = 1, 2, \cdots, N), \ (15)$$

where $h_i(\boldsymbol{f}) = \tau_i - \boldsymbol{a}_i^T \boldsymbol{f}$ and $g_j(\boldsymbol{f}) = -f_j$. $\boldsymbol{a}_j \in \Re^N$ is a column vector of $\boldsymbol{A}$. Recall

$$q_j \triangleq \frac{\partial u(\boldsymbol{f})}{\partial f_j} = rc_j f_j^{r-1}, (j = 1, \cdots, N) \ (16)$$

$$\frac{\partial h_i(\boldsymbol{f})}{\partial f_j} = a_{ij}, \quad (17)$$

$$\frac{\partial g_{j_1}}{\partial f_{j_2}} = \begin{cases} -1, & j_1 = j_2 \\ 0, & j_1 \neq j_2 \end{cases}. \quad (18)$$

Therefore, (13) is written as

$$\boldsymbol{q} = w(\boldsymbol{f}) = \boldsymbol{A}^T \boldsymbol{\mu} + \boldsymbol{\lambda} \quad (19)$$

where $\boldsymbol{q} = [q_1, \cdots, q_N]^T$, $\boldsymbol{\mu} = [\mu_1, \cdots, \mu_M]^T$, and $\boldsymbol{\lambda} = [\lambda_1, \cdots, \lambda_N]^T$. From (15), $\lambda_j = 0$ if $f_j > 0$. Using (4) and (6), (19) can be rewritten as

$$\begin{bmatrix} \boldsymbol{q}_t \\ \boldsymbol{q}_n \\ \hline \boldsymbol{0} \end{bmatrix} = \begin{bmatrix} \boldsymbol{A}_t \\ \boldsymbol{A}_n \\ \hline \boldsymbol{A}_v \end{bmatrix} \boldsymbol{\mu} + \begin{bmatrix} \boldsymbol{0} \\ \boldsymbol{0} \\ \hline \boldsymbol{\lambda}_v \end{bmatrix}. \quad (20)$$

For the normal muscle force $\boldsymbol{f}_0(= w^{-1}(\boldsymbol{q}_0))$, (20) will be

$$\boldsymbol{q}_0 = \boldsymbol{A}^T \boldsymbol{\mu}_0 + \boldsymbol{\lambda}_0 \rightarrow \begin{bmatrix} \boldsymbol{q}_{0t} \\ \boldsymbol{q}_{0n} \\ \hline \boldsymbol{0} \end{bmatrix} = \begin{bmatrix} \boldsymbol{A}_t \\ \boldsymbol{A}_n \\ \hline \boldsymbol{A}_v \end{bmatrix} \boldsymbol{\mu}_0 + \begin{bmatrix} \boldsymbol{0} \\ \boldsymbol{0} \\ \hline \boldsymbol{\lambda}_{0v} \end{bmatrix}. \quad (21)$$

Similarly, for the desired muscle force $\boldsymbol{f}_d(= w^{-1}(\boldsymbol{q}_d))$,

$$\boldsymbol{q}_d = \boldsymbol{A}^T \boldsymbol{\mu}_d + \boldsymbol{\lambda}_d \rightarrow \begin{bmatrix} \boldsymbol{q}_{dt} \\ \boldsymbol{q}_{dn} \\ \hline \boldsymbol{0} \end{bmatrix} = \begin{bmatrix} \boldsymbol{A}_t \\ \boldsymbol{A}_n \\ \hline \boldsymbol{A}_v \end{bmatrix} \boldsymbol{\mu}_d + \begin{bmatrix} \boldsymbol{0} \\ \boldsymbol{0} \\ \hline \boldsymbol{\lambda}_{dv} \end{bmatrix}. \quad (22)$$

Let $\boldsymbol{\mu}_d = \boldsymbol{\mu}_0 + \boldsymbol{\alpha}, \boldsymbol{\lambda}_{dv} = \boldsymbol{\lambda}_{0v} - \boldsymbol{A}_v \boldsymbol{\alpha}$ where $\boldsymbol{\alpha}$ is a control input vector in the Kuhn-Tucker form. $\boldsymbol{q}_d$ can be represented as

$$\begin{aligned} \boldsymbol{q}_d &= \begin{bmatrix} \boldsymbol{q}_{dt} \\ \boldsymbol{q}_{dn} \\ \hline \boldsymbol{0} \end{bmatrix} = \begin{bmatrix} \boldsymbol{q}_{0t} \\ \boldsymbol{q}_{0n} \\ \hline \boldsymbol{0} \end{bmatrix} + \begin{bmatrix} \boldsymbol{A}_t \\ \boldsymbol{A}_n \\ \hline \boldsymbol{A}_v \end{bmatrix} \boldsymbol{\alpha} \\ &= \left(\begin{bmatrix} \boldsymbol{A}_t \\ \boldsymbol{A}_n \\ \hline \boldsymbol{A}_v \end{bmatrix} \boldsymbol{\mu}_0 + \begin{bmatrix} \boldsymbol{0} \\ \boldsymbol{0} \\ \hline \boldsymbol{\lambda}_{0v} \end{bmatrix} \right) + \left(\begin{bmatrix} \boldsymbol{A}_t \\ \boldsymbol{A}_n \\ \hline \boldsymbol{A}_v \end{bmatrix} \boldsymbol{\alpha} + \begin{bmatrix} \boldsymbol{0} \\ \boldsymbol{0} \\ \hline -\boldsymbol{A}_v \boldsymbol{\alpha} \end{bmatrix} \right) \\ &= \begin{bmatrix} \boldsymbol{A}_t \\ \boldsymbol{A}_n \\ \hline \boldsymbol{A}_v \end{bmatrix} (\boldsymbol{\mu}_0 + \boldsymbol{\alpha}) + \begin{bmatrix} \boldsymbol{0} \\ \boldsymbol{0} \\ \hline \boldsymbol{\lambda}_{0v} - \boldsymbol{A}_v \boldsymbol{\alpha} \end{bmatrix} \end{aligned} \quad (23)$$

From the first row of (23) provides the condition to completely realize the desired forces for the target muscles, i.e.,

$$\boldsymbol{q}_{td} - \boldsymbol{q}_{t0} = w(\boldsymbol{f}_{td}) - w(\boldsymbol{f}_{t0}) = \boldsymbol{A}_t \boldsymbol{\alpha}. \quad (24)$$

A solution for $\boldsymbol{\alpha}$ exists if the following condition holds:

$$\text{rank}(\ \boldsymbol{A}_t\ ) = \text{rank}(\ \begin{bmatrix} \boldsymbol{A}_t & w(\boldsymbol{f}_{td}) - w(\boldsymbol{f}_{t0}) \end{bmatrix}\ ) \quad (25)$$

which gives the condition 1).

To maintain inactive muscles inactive after muscle-force control, $\boldsymbol{\lambda}_{dv} > \boldsymbol{0}$ must be satisfied. Therefore,

$$\begin{aligned} \boldsymbol{\lambda}_{dv} &= \boldsymbol{\lambda}_{0v} - \boldsymbol{A}_v \boldsymbol{\alpha} \\ &= -\boldsymbol{A}_v \begin{bmatrix} \boldsymbol{A}_t \\ \boldsymbol{A}_n \end{bmatrix}^+ \begin{bmatrix} \boldsymbol{q}_{0t} \\ \boldsymbol{q}_{0n} \end{bmatrix} - \boldsymbol{A}_v \boldsymbol{\alpha} > \boldsymbol{0} \end{aligned} \quad (26)$$

which gives the condition 2).

To maintain non-target muscles positive, i.e., $\boldsymbol{f}_{nd}$, the condition is obtained from the second row of (23) as follows:

$$w(\boldsymbol{f}_{nd}) = \boldsymbol{A}_n \boldsymbol{\alpha} + w(\boldsymbol{f}_{n0}) > \boldsymbol{0} \quad (27)$$

which is the condition 3).

The solution of (24) is given by

$$\boldsymbol{\alpha} = \boldsymbol{A}_t^+ [w(\boldsymbol{f}_{td}) - w(\boldsymbol{f}_{t0})] + (\boldsymbol{I} - \boldsymbol{A}_t^+ \boldsymbol{A}_t) \boldsymbol{\beta} \quad (28)$$

where $\boldsymbol{\beta}$ is a free parameter that indicates the redundancy of the solution; $\boldsymbol{\beta}$ determines the distribution of resultant non-target muscle forces while maintaining the complete realization of desired forces for target muscles. Note that the choice of $\boldsymbol{\beta}$ is generally arbitrary. One reasonable choice may be to minimize the change of non-target muscles. The change of non-target muscles is represented by

$$\begin{aligned} \Delta \boldsymbol{f}_n &= w(\boldsymbol{f}_{nd}) - w(\boldsymbol{f}_{n0}) = \boldsymbol{A}_n \boldsymbol{\alpha} \\ &= \boldsymbol{A}_n \{ \boldsymbol{A}_t^+ [w(\boldsymbol{f}_{td}) - w(\boldsymbol{f}_{t0})] + (I - \boldsymbol{A}_t^+ \boldsymbol{A}_t) \boldsymbol{\beta} \} \\ &= \boldsymbol{A}_n \boldsymbol{A}_t^+ [w(\boldsymbol{f}_{td}) - w(\boldsymbol{f}_{t0})] - [-\boldsymbol{A}_n(I - \boldsymbol{A}_t^+ \boldsymbol{A}_t)] \boldsymbol{\beta} \end{aligned}$$
$$\quad (29)$$

Therefore, the following $\boldsymbol{\beta}$ minimizes $||\Delta \boldsymbol{f}_n||$ to avoid unnecessary influences on non-target muscles:

$$\boldsymbol{\beta} = [-\boldsymbol{A}_n(\boldsymbol{I} - \boldsymbol{A}_t^+ \boldsymbol{A}_t)]^+ \boldsymbol{A}_n \boldsymbol{A}_t^+ [w(\boldsymbol{f}_{td}) - w(\boldsymbol{f}_{t0})] \quad (30)$$

At the level of individual muscle forces, the following changes are created for the target and non-target muscles:

$$w^{-1} \left(\begin{bmatrix} \boldsymbol{q}_{dt} \\ \boldsymbol{q}_{dn} \end{bmatrix} - \begin{bmatrix} \boldsymbol{q}_{0t} \\ \boldsymbol{q}_{0n} \end{bmatrix} \right) = w^{-1} \left(\begin{bmatrix} \boldsymbol{A}_t \\ \boldsymbol{A}_n \end{bmatrix} \boldsymbol{\alpha} \right). \quad (31)$$

Therefore, the corresponding torques given by (9) need to be externally applied at the joint level.

REFERENCES

[1] P. Davies, *Steps to Follow: The Comprehensive Treatment of Patients with Hemiplegia.* Springer, 2000.

[2] V. Krishnamoorthy, J. Scholz, and M. Latash, "The use of flexible arm muscle synergies to perform an isometric stabilization task," *Clinical Neurophysiology*, vol. 118, no. 3, pp. 525–537, 2007.

[3] D. Reisman and J. Scholz, "Aspects of joint coordination are preserved during pointing in persons with post-stroke hemiparesis." *Brain*, vol. 126, no. 11, p. 2510, 2003.

[4] RD. Crowninshield, et al., "A physiologically based criterion of muscle force prediction in locomotion," *J. Biomechanics*, vol. 14, pp. 793–801, 1981.

[5] B. van Bolhuis and C. Gielen, "A comparison of models explaining muscle activation patterns for isometric contractions," *Biological Cybernetics*, vol. 81, no. 3, pp. 249–261, 1999.

[6] T. Buchanan and D. Shreeve, "An Evaluation of Optimization Techniques for the Prediction of Muscle Activation Patterns During Isometric Tasks," *Journal of Biomechanical Engineering*, vol. 118, p. 565, 1996.

[7] B. Prilutsky, "Coordination of two-and one-joint muscles: functional consequences and implications for motor control," *Motor Control*, vol. 4, no. 1, pp. 48–52, 2000.

[8] S. Delp, J. Loan, M. Hoy, F. Zajac, E. Topp, J. Rosen, V. Center, and P. Alto, "An interactive graphics-based model of the lower extremity to studyorthopaedic surgical procedures," *Biomedical Engineering, IEEE Transactions on*, vol. 37, no. 8, pp. 757–767, 1990.

[9] D. Karlsson and B. Peterson, "Towards a model for force predictions in the human shoulder," *Journal of biomechanics*, vol. 25, no. 2, pp. 189–199, 1992.

[10] H. Veeger, F. Van der Helm, L. Van der Woude, G. Pronk, and R. Rozendal, "Inertia and muscle contraction parameters for musculoskeletal modelling of the shoulder mechanism," *J Biomech*, vol. 24, no. 7, pp. 615–29, 1991.

[11] J. Biggs and K. Horch, "A three-dimensional kinematic model of the human long finger and the muscles that actuate it," *Medical Engineering and Physics*, vol. 21, no. 9, pp. 625–639, 1999.

[12] W. Maurel and D. Thalmann, "A Case Study on Human Upper Limb Modelling for Dynamic Simulation," *Computer Methods in Biomechanics and Biomedical Engineering*, vol. 2, no. 1, pp. 65–82, 1999.

[13] F. Martini and E. Bartholomew, *Essentials of Anatomy & Physiology*. Prentice Hall, 2000.

[14] A. Hamilton, K. Jones, and D. Wolpert, "The scaling of motor noise with muscle strength and motor unit number in humans," *Exp Brain Res*, vol. 157, pp. 417–430, 2004.

[15] R. Osu, N. Kamimura, H. Iwasaki, E. Nakano, C. Harris, Y. Wada, and M. Kawato, "Optimal Impedance Control for Task Achievement in the Presence of Signal-Dependent Noise," *Journal of Neurophysiology*, vol. 92, no. 2, pp. 1199–1215, 2004.

[16] D. Nozaki, K. Nakazawa, and M. Akai, "Muscle Activity Determined by Cosine Tuning With a Nontrivial Preferred Direction During Isometric Force Exertion by Lower Limb," *Journal of Neurophysiology*, vol. 93, no. 5, pp. 2614–2624, 2005.

[17] J. Ueda, M. Ding, M. Matsugashita, R. Oya, and T. Ogasawara, "Pinpointed control of muscles by using power-assisting device," in *2007 IEEE International Conference on Robotics and Automation*, 2007, pp. 3621–3626.

[18] J. Ueda, M. Matsugashita, R. Oya, and T. Ogasawara, "Control of muscle force during exercise using a musculoskeletal-exoskeletal integrated human model," in *10th International Symposium on Experimental Robotics(ISER2006)*, Rio de Janeiro, Brazil, 2006.

[19] D. Ming, J. Ueda, and T. Ogasawara, "Pinpointed muscle force control using a power-assisting device: System configuration and experiment," *Biomedical Robotics and Biomechatronics, 2008. BioRob 2008. 2nd IEEE RAS & EMBS International Conference on*, pp. 181–186, Oct. 2008.

[20] J. Ueda, M. Hyderabadwala, V. Krishnamoorthy, and M. Shinohara, "Motor task planning for neuromuscular function tests using an individual muscle control technique," *IEEE 11th International Conference on Rehabilitation Robotics*, 2009.

[21] H. Krebs, N. Hogan, M. Aisen, and B. Volpe, "Robot-aided neurorehabilitation," *IEEE transactions on rehabilitation engineering: a publication of the IEEE Engineering in Medicine and Biology Society*, vol. 6, no. 1, p. 75, 1998.

[22] B. Volpe, P. Huerta, J. Zipse, A. Rykman, D. Edwards, L. Dipietro, N. Hogan, and H. Krebs, "Robotic Devices as Therapeutic and Diagnostic Tools for Stroke Recovery," *Archives of Neurology*, vol. 66, no. 9, p. 1086, 2009.

[23] A. Toth, G. Arz, G. Fazekas, D. Bratanov, and N. Zlatov, "Post stroke shoulder-elbow physiotherapy with industrial robots," *Lecture notes in control and information sciences*, pp. 391–411, 2004.

[24] M. Alexander, M. Nelson, and A. Shah, "Orthotics, adapted seating and assistive devices," *Pediatric Rehabilitation*, pp. 186–187, 1992.

[25] S. Lee and Y. Sankai, "Power assist control for walking aid with HAL-3 based on EMG and impedance adjustment around knee joint," in *Intelligent Robots and System, 2002. IEEE/RSJ International Conference on*, vol. 2, 2002.

[26] N. Tsagarakis and D. Caldwell, "Development and Control of a Soft-ActuatedExoskeleton for Use in Physiotherapy and Training," *Autonomous Robots*, vol. 15, no. 1, pp. 21–33, 2003.

[27] D. Ferris, K. Gordon, G. Sawicki, and A. Peethambaran, "An improved powered ankle-foot orthosis using proportional myoelectric control," *Gait & Posture*, vol. 23, no. 4, pp. 425–428, 2006.

[28] J. Rosen, M. Fuchs, and M. Arcan, "Performances of Hill-type and neural network muscle models-toward a myosignal-based exoskeleton," *Computers and Biomedical Research*, vol. 32, no. 5, pp. 415–439, 1999.

[29] R. Sanchez, J. Liu, S. Rao, P. Shah, R. Smith, T. Rahman, S. Cramer, J. Bobrow, and D. Reinkensmeyer, "Automating arm movement training following severe stroke: functional exercises with quantitative feedback in a gravity-reduced environment." *IEEE transactions on neural systems and rehabilitation engineering: a publication of the IEEE Engineering in Medicine and Biology Society*, vol. 14, no. 3, pp. 378–389, 2006.

[30] G. Colombo, M. Joerg, R. Schreier, and V. Dietz, "Treadmill training of paraplegic patients using a robotic orthosis." *Journal of rehabilitation research and development*, vol. 37, no. 6, pp. 693–700, 2000.

[31] T. Nef, M. Mihelj, and R. Riener, "ARMin: a robot for patient-cooperative arm therapy," *Medical and Biological Engineering and Computing*, vol. 45, no. 9, pp. 887–900, 2007.

[32] J. Veneman, R. Kruidhof, E. Hekman, R. Ekkelenkamp, E. Van Asseldonk, and H. van der Kooij, "Design and Evaluation of the LOPES Exoskeleton Robot for Interactive Gait Rehabilitation," *IEEE Transactions On Neural Systems And Rehabilitation Engineering*, vol. 15, no. 3, p. 379, 2007.

[33] H. Kazerooni, "Extender: A case study for human-robot, interaction via transfer of power and information signals," *Proc. IEEE Int. Workshop on Robot and Human Communication*, pp. 10–20, 1993.

[34] H. Kazerooni, J. Racine, L. Huang, and R. Steger, "On the Control of the Berkeley Lower Extremity Exoskeleton (BLEEX)," in *IEEE International Conference on Robotics and Automation*, vol. 4, 2005, pp. 4353–4360.

[35] L. Dipietro, M. Ferraro, J. Palazzolo, H. Krebs, B. Volpe, and N. Hogan, "Customized interactive robotic treatment for stroke: EMG-triggered therapy," *IEEE transactions on neural systems and rehabilitation engineering: a publication of the IEEE Engineering in Medicine and Biology Society*, vol. 13, no. 3, p. 325, 2005.

[36] G. Yamaguchi, *Dynamic modeling of musculoskeletal motion*. Kluwer Academic Publishers, 2001.

[37] M. Lemay and P. Crago, "A dynamic model for simulating movements of the elbow, forearm, and wrist," *Journal of biomechanics*, vol. 29, no. 10, pp. 1319–1330, 1996.

[38] P. Pardalos and J. Rosen, *Constrained global optimization: algorithms and applications*, 1987.

[39] D. Bertsekas, *Nonlinear programming*. Athena Scientific Belmont, Mass, 1999.

[40] MotCo Project, "http://motco.info/data/pcsa.html."